

Supplement of Atmos. Meas. Tech., 12, 6079–6089, 2019
<https://doi.org/10.5194/amt-12-6079-2019-supplement>
© Author(s) 2019. This work is distributed under
the Creative Commons Attribution 4.0 License.



Supplement of

A new laser-based and ultra-portable gas sensor for indoor and outdoor formaldehyde (HCHO) monitoring

Joshua D. Shutter et al.

Correspondence to: Joshua D. Shutter (shutter@g.harvard.edu)

The copyright of individual parts of the supplement might differ from the CC BY 4.0 License.

Table S1. Frequencies and line intensities of HITRAN lines used by HAPP fits

| Wavenumber / cm ⁻¹ | Molecular species | Spectral line intensity (296 K) / cm ⁻¹ / molecule · cm ⁻² |
|----------------------------------|-----------------------|---|
| 2831.2598 | CH ₄ | 2.863e-22 |
| 2831.2701 | CH ₄ | 2.308e-25 |
| 2831.2737 | HCHO | 2.101e-20 |
| 2831.2780 | CH ₄ | 2.471e-22 |
| 2831.2802 | CH ₄ | 3.408e-25 |
| 2831.3160 | CH ₄ | 3.394e-23 |
| 2831.3259 | HCHO | 2.900e-21 |
| 2831.3366 | CH ₄ | 2.603e-25 |
| 2831.3501 | CH ₄ | 3.240e-25 |
| 2831.3550 | HCHO | 1.420e-20 |
| 2831.3657 | CH ₄ | 3.587e-25 |
| 2831.4055 | HDO | 1.812e-28 |
| 2831.4097 | HDO | 1.812e-28 |
| 2831.4209 | CH₄ | 1.553e-23 |
| 2831.5393 | HCHO | 5.622e-21 |
| 2831.5534 | CH ₄ | 8.870e-25 |
| 2831.5576 | HCHO | 5.543e-21 |
| 2831.5616 | CH₄ | 1.549e-23 |
| 2831.5801 | HDO | 4.140e-28 |
| 2831.6413 | HCHO | 5.839e-20 |
| 2831.6879 | HCHO | 1.499e-21 |
| 2831.6892 | HCHO | 1.499e-21 |
| 2831.6961 | CH ₄ | 6.671e-25 |
| 2831.6989 | HCHO | 1.410e-20 |
| 2831.8134 | HCHO | 6.509e-21 |
| 2831.8214 | CH ₄ | 3.671e-24 |
| 2831.8413 | HDO | 3.014e-24 |
| 2831.8516 | CH ₄ | 1.983e-24 |
| 2831.8906 | HDO | 9.812e-28 |
| 2831.8948 | H ₂ O | 1.595e-28 |
| 2831.9199 | CH₄ | 1.622e-21 |
| 2831.9569 | HDO | 2.713e-27 |

Spectral lines from the same molecular species are fitted together rather than independently. Lines bolded in blue were used in experiments that utilized ultra-zero air, and it was discovered that all the lines listed produced a more superior fit than only the lines bolded in blue when sampling ambient air. Spectral frequencies and line intensities were accessed using HITRAN on the Web (<http://hitran.iao.ru/>) (Rothman et al., 2013).

Table S2. 1σ standard deviation for Aeris sensor at various integration times. All values are in pptv and were obtained by either (1) bubbling ultra-zero air (1000 sccm) through water (HDO mode) or (2) adding chemically-pure 99.5% CH_4 (< 1 sccm) to 5000 sccm ultra-zero air (CH_4 mode).

| Integration time / s | ART fit HDO mode / pptv HCHO | HAPP fit HDO mode / pptv HCHO | Average of the two HDO modes / pptv HCHO | HAPP fit CH_4 mode / pptv HCHO |
|----------------------|------------------------------------|-------------------------------------|--|---|
| 30 | 1200 | 1000 | 700 | 1350 |
| 60 | 1000 | 800 | 660 | 1100 |
| 120 | 730 | 600 | 530 | 720 |
| 300 | 430 | 380 | 330 | 460 |
| 900 | 230 | 190 | 180 | 320 |
| 1800 | 160 | 140 | 120 | 280 |
| 3600 | 140 | 100 | 100 | 230 |
| 7200 | 160 | 110 | 110 | 140 |
| 20000 | 170 | 160 | 160 | 200 |

5

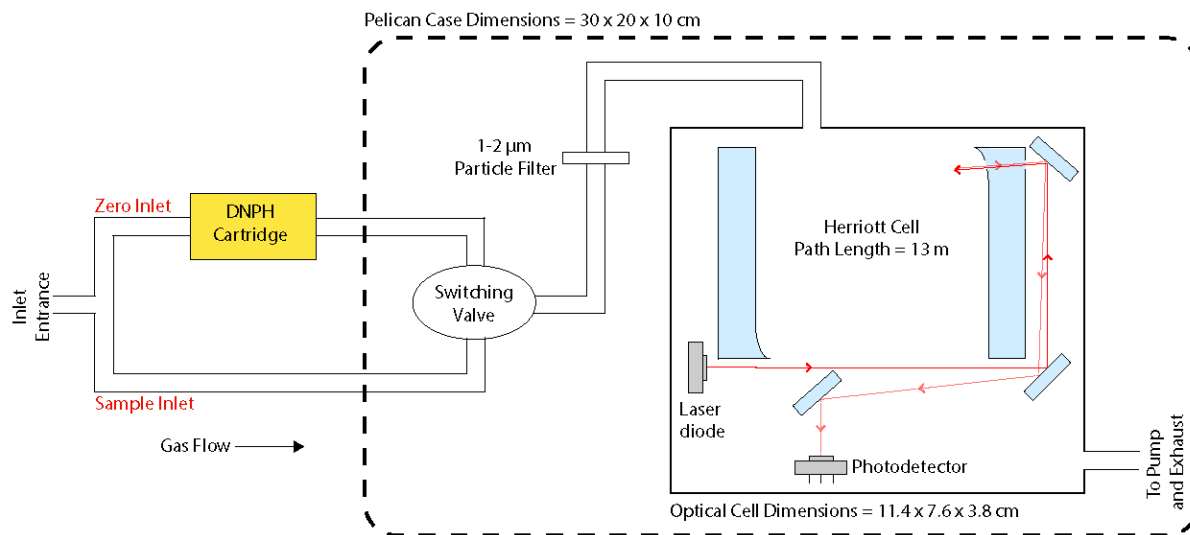
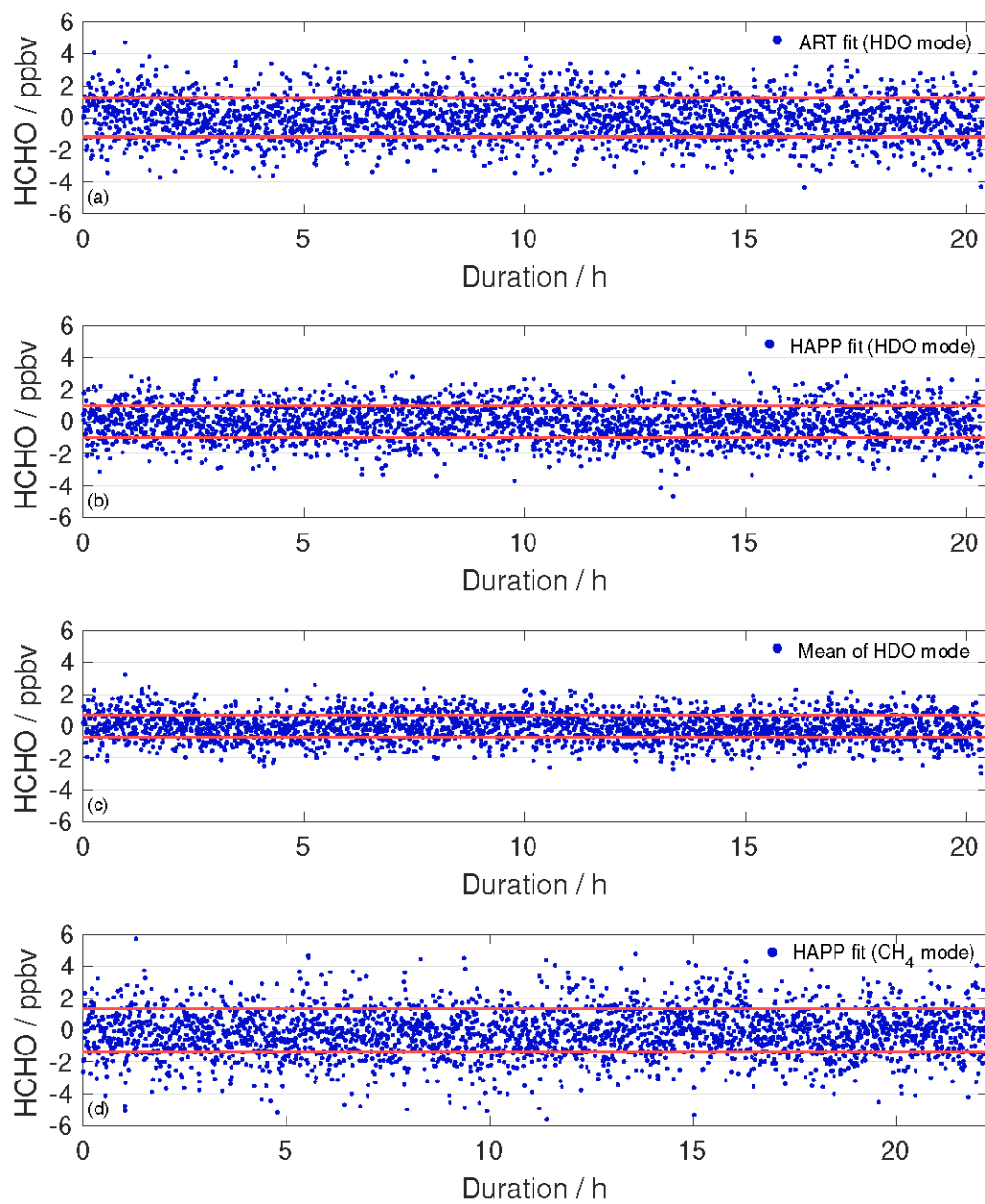


Figure S1. Schematic diagram of the Aeris sensor. Air flows through the inlet entrance, and the switching valve either allows air to pass directly into the instrument via the sample inlet or is first scrubbed of HCHO via the zero inlet. Before entering the Herriott cell, all dust is removed from the air flow with a 1-2 μm particle filter. The patented folded Herriott cell (US Patent #10,222,595) has a path length of 13 m and dimensions of 11.4 x 7.6 x 3.8 cm (Paul, 2019). The laser diode, photodetector, filters, and mirror coatings are proprietary information.

15



5 Figure S2. Raw time series data used to derive the Allan-Werle deviation curves in Figure 3. All points shown have an integration time of 30 s and were obtained by flowing ultra zero air through the Aeris sensor for a minimum of 20 h. Red lines indicate $\pm 1\sigma$ standard deviation from the mean of the data. Raw data for (a) ART fit (HDO mode), (b) HAPP fit (HDO mode), (c) mean of HDO fits, and (d) HAPP fit (CH_4 mode).

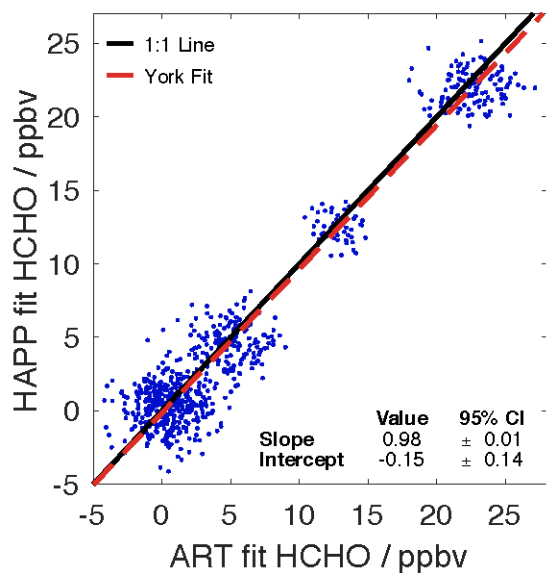


Figure S3. Correlation plot between the Aeris Real-time (ART) fit and the Harvard Aeris-Post Processing (HAPP) fit ($R^2 = 0.941$).

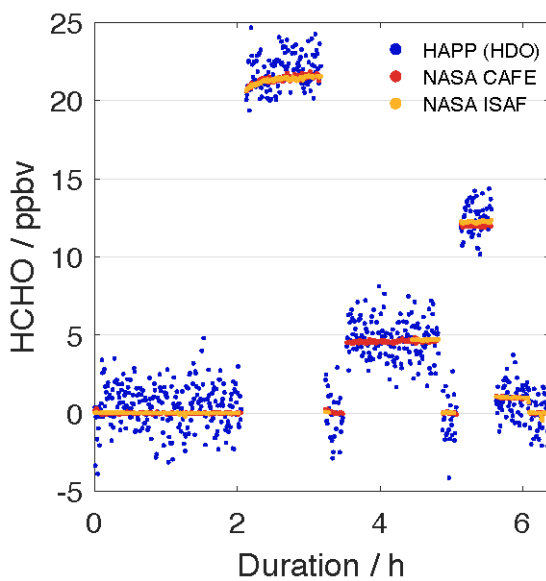


Figure S4. Time series showing the HCHO mixing ratios from the Aeris sensor (HAPP HDO fit) and NASA ISAF and CAFE during a multi-hour stepped intercomparison performed at NASA Goddard in November 2017. All data are reported with an integration time of 30 s.

Paul, J. B.: Compact Folded Optical Multipass System, US Patent #10,222,595. 2019.

Rothman, L. S., Gordon, I. E., Babikov, Y., Barbe, A., Benner, D. C., Bernath, P. F., Birk, M., Bizzocchi, L., Boudon, V., Brown, L. R., Campargue, A., Chance, K., Cohen, E. A., Coudert, L. H., Devi, V. M., Drouin, B. J., Fayt, A., Flaud, J.-M., Gamache, R. R., Harrison, J. J., Hartmann, J.-M., Hill, C., Hodges, J. T., Jacquemart, D., Jolly, A., Lamouroux, J., Le Roy, R. J., Li, G., Long, D. A., Lyulin, O. M., Mackie, C. J., Massie, S. T., Mikhailenko, S., Müller, H. S. P., Naumenko, O. V., Nikitin, A. V., Orphal, J., Perevalov, V., Perrin, A., Polovtseva, E. R., Richard, C., Smith, M. A. H., Starikova, E., Sung, K., Tashkun, S., Tennyson, J., Toon, G. C., Tyuterev, V. G. and Wagner, G.: The HITRAN2012 molecular spectroscopic database, *J. Quant. Spectrosc. Radiat. Transf.*, 130, 4–50, doi:10.1016/J.JQSRT.2013.07.002, 2013.